Coarsening and aging of lattice polymers: Influence of bond fluctuations

Henrik Christiansen, Suman Majumder, and Wolfhard Janke

AIP | The Journal of Chemical Physics

PERSPECTIVES

Coarsening and aging of lattice polymers: Influence of bond fluctuations

Henrik Christiansen,[a] Suman Majumder,[b] and Wolfhard Janke[c]
Institut für Theoretische Physik, Universität Leipzig, Postfach 100 920, 04009 Leipzig, Germany

We present results for the nonequilibrium dynamics of collapse for a model flexible homopolymer on simple cubic lattices with fixed and fluctuating bonds between the monomers. Results from our Monte Carlo simulations show that, phenomenologically, the sequence of events observed during the collapse are independent of the bond criterion. While the growth of the clusters (of monomers) at different temperatures exhibits a non-universal power-law behavior when the bonds are fixed, the introduction of fluctuations in the bonds by considering the existence of diagonal bonds produces a temperature independent growth, which can be described by a universal nonequilibrium finite-size scaling function with a non-universal metric factor. We also examine the related aging phenomenon, probed by a suitable two-time density-density autocorrelation function showing a simple power-law scaling with respect to the growing cluster size. Unlike the cluster-growth exponent α_c, the nonequilibrium autocorrelation exponent λ_C governing the aging during the collapse, however, is independent of the bond type and strictly follows the bounds proposed by Majumder and Janke [Phys. Rev. E **93**, 032506 (2016)] at all temperatures. *Published by AIP Publishing.* [http://dx.doi.org/10.1063/1.4991667]

I. INTRODUCTION

Despite their apparent extreme simplification, lattice models have been proved to be very handy in Monte Carlo (MC) simulations[1] providing useful insights into problems related to various phase transitions, e.g., gas-liquid transition,[2] ferromagnetic transition,[3] collapse transition of a polymer,[4–6] etc. In particular, the behavior of the static properties obtained from such simulations of lattice models has been found to be in fairly good agreement with the corresponding theories and often with experiments. However, the dynamic properties seem to be largely dependent on the choice of the model as well as the implemented "local moves." In this paper, we aim to understand similar effects in the nonequilibrium dynamics of the collapse transition of lattice polymers.

Collapse transition refers to the change in conformation that a polymer chain, initially in an expanded coil state under good solvent conditions (or high temperature), experiences when transferred to a bad solvent (low temperature), where the equilibrium conformation is globular in nature.[7,8] The significance of such collapse transition lies in its close association with the folding process of certain macromolecules like proteins.[9,10] Ever since its introduction, self-avoiding walks (SAW) on lattices[11] have been successfully used to obtain the critical exponent ν related to the size of the polymer,[12] i.e., the radius of gyration $R_g \sim N^\nu$, where N is the number of monomers in the polymer chain. Furthermore, by introducing an attractive interaction for the nearest-neighbor non-bonded contacts, and conducting MC simulations of such interactive self-avoiding walk (ISAW) on lattices, one can capture the collapse transition as well as the freezing or crystallization.[6,13] Thus, on the one hand, the static properties of a polymer in equilibrium have been quite well studied using lattice as well as off-lattice models. On the other hand, the dynamic properties have received less attention. For dynamic studies of polymers, there is a quest[14] for a suitable model and appropriate set of moves that reproduces the well-known Rouse dynamics in equilibrium,[15] valid in the absence of hydrodynamics. These led to the introduction of bond-fluctuation models[16] and diagonal bond models[17,18] that not only reproduce the static properties correctly but also provide reliable dynamics. However, the application of such lattice models to understand the nonequilibrium kinetics of the collapse transition has rarely been attempted.

Current developments in experimental techniques have made it a lot easier to monitor a single polymer,[19,20] in turn urging more interests in the dynamics of a single polymer via computer simulations. In this regard, one can understand the collapse dynamics of a homopolymer[21–23] by drawing analogies with usual nonequilibrium coarsening phenomena of particle or spin systems.[24,25] Especially, the scaling of the growth of monomer clusters formed during the collapse and the scaling of the two-time density-density autocorrelation functions (showing aging) are worth mentioning. Phenomenologically, the events that occur during the collapse can be well described by the "pear-necklace" picture of Halperin and Goldbart (HG).[26] In accordance with HG, confirmed both in lattice[27] and off-lattice simulations (both without hydrodynamics[21,23] and with hydrodynamics[28,29]), the polymer collapse starts with the formation of small clusters along the chain at locally higher densities. Those clusters subsequently become stable and start to coarsen by accumulating monomers from the connecting bridges. Once those bridges stiffen, clusters start to coalesce with each other until only a single globular cluster is left. Finally, the monomers within the globule rearrange

a)Electronic mail: henrik.christiansen@itp.uni-leipzig.de
b)Electronic mail: suman.majumder@itp.uni-leipzig.de
c)Electronic mail: wolfhard.janke@itp.uni-leipzig.de

to form an even more compact configuration, minimizing the surface energy. The growth of the clusters during the coarsening or coalescence phase of the collapse can be viewed under the light of well-known ordering or coarsening kinetics. In earlier studies, the cluster growth was shown to follow a simple power law: $C_s(t) \sim t^{\alpha_c}$ (where $C_s(t)$ is the cluster size at time t), and the cluster-growth exponent α_c was found to be 1/2 for lattice polymers[27] and $\alpha_c = 2/3$ for an off-lattice model,[30] consistent with a Gaussian self-consistent theory.[31] However, recently, in an off-lattice model[21,23] with diffusive dynamics (in the absence of hydrodynamics) it has been shown that the average cluster size, $C_s(t)$, obeys a scaling of the form

$$C_s(t) = C_0 + At^{\alpha_c}, \tag{1}$$

where C_0 is the crossover (from the initial cluster-formation stage to the coarsening stage) cluster size. The corresponding growth exponent for this model is $\alpha_c \approx 1$, as observed for Ostwald ripening.[32] Moreover, using the scaling form (1) of the cluster growth, it has been shown that α_c is independent of the quench temperatures and the growth can be described by a universal nonequilibrium finite-size scaling function with a non-universal metric factor.[23]

In analogy with the nonequilibrium ordering or coarsening processes of particle or spin systems, another intriguing feature observed during the collapse is the presence of aging,[33,34] generally probed by a two-time density-density autocorrelation function $C(t, t_w)$ (where t is the observation time and t_w is the waiting time). In this context, one is particularly interested in the related dynamic scaling given as

$$C(t, t_w) = A_C x_C^{-\lambda_C}; \ x_C = \frac{C_s(t)}{C_s(t_w)}. \tag{2}$$

Such power-law scaling is reminiscent of the scaling observed in the Ising model with both nonconserved[35–41] and conserved[42] order parameter, where the two-time order-parameter autocorrelation function scales with the ratio of the length scales at the concerned times. In Refs. 22 and 23, for collapse in an off-lattice model, it has been shown that the value of the nonequilibrium autocorrelation exponent $\lambda_C \approx 1.25$ in (2) is independent of the quench temperature and obeys a theoretically predicted bound[22]

$$(\nu d - 1) \leq \lambda_C \leq 2(\nu d - 1), \tag{3}$$

where d is the dimension and ν is the previously discussed static critical exponent related to the size of the polymer. Such a dimension-dependent bound was first proposed for aging in ordering spin glasses[35] and later verified for spin systems having nonconserved order-parameter dynamics.[37] A more general and in fact sharpened bound that also includes the conserved order-parameter dynamics case was later proposed in Ref. 43. The bound (3), too, is general for the collapse of a polymer and, although not yet verified, expected to be valid in the presence of hydrodynamics as well.

In spite of the simplicity of implementation, the investigation of the above-mentioned scaling laws related to the nonequilibrium dynamics of collapse transition using a lattice model has been ignored so far. Motivated by that, we present comparative results from MC simulations of two different lattice models with fixed and fluctuating bonds. With the primary focus on the various scaling laws related to the collapse, we show that while the model with fixed bonds does not provide a universal picture of the cluster growth, the model with fluctuating bonds yields a scaling independent of the quench temperature. However, the scaling (2) related to aging is independent of the models considered, indicating a dynamic universal behavior of aging.

The rest of the paper is organized in the following manner. Next, in Sec. II, we describe the models and the method of simulation used. Then, in Sec. III, we present our main results concerning the cluster growth and aging followed by a discussion and conclusion in Sec. IV.

II. MODELS AND METHOD

For our polymer model we consider an ISAW on a simple cubic lattice with unit lattice constant, fixing the unit of length. In this model each lattice site can be occupied by a single monomer. The energies leading to the collapse transition are governed by the Hamiltonian,

$$H = -\frac{1}{2} \sum_{i \neq j, j \pm 1} w(r_{ij}), \tag{4}$$

where i and j correspond to a non-bonded pair of monomers, r_{ij} is the Euclidean distance between them, and $w(r_{ij})$ is the distance-dependent interaction parameter. We use the simplest case of nearest-neighbor interaction as

$$w(r_{ij}) = \begin{cases} \epsilon & r_{ij} = 1 \\ 0 & \text{else} \end{cases}. \tag{5}$$

For computational convenience and comparability to previous works,[6,44] we choose $\epsilon = 1$, which sets the energy, respectively, the temperature scales (the unit of temperature is ϵ/k_B, where the Boltzmann factor k_B is set to unity). The Hamiltonian given by (4) and (5) favors at low temperature more and more nearest-neighbor non-bonded contacts, thus facilitating a coil-globule transition in the model. For our studies, we use two different criteria for the bonds connecting the adjacent monomers. In one case, we fix the bond distances to 1, which from now on we refer to as Model I. In the other case we allow a fluctuation in the bond length by additionally considering diagonal bonds, i.e., there the possible bond lengths are 1, $\sqrt{2}$, and $\sqrt{3}$. This we refer to as Model II. Note that in both cases the attractive interaction (5) only acts between monomers located at nearest-neighbor sites. The thermodynamic properties of Model I are well studied for both the freezing and collapse transition.[6] Model II has its origin from the bond-fluctuation model of Carmesin and Kremer[16] and has been independently studied both for the static and dynamic properties in equilibrium.[17,18,45]

We introduce the dynamics in the models via Markov chain Monte Carlo simulation. For Model I a trial move of a randomly picked monomer in the chain could be an end-move, corner-move, or the crankshaft-move, depending on the position of the monomer. Care has to be taken to preserve the excluded volume condition (no two monomers can occupy the same lattice site) and to maintain the bond

connectivity between adjacent monomers. Since in Model II we allow a fluctuation in the bond length, a trial move only consists of local displacement of a randomly picked monomer with the constraint of preserving the excluded volume condition and the bond connectivity. For details on the allowed moves in Model II, we refer to Ref. 18. For both the models, a trial move is accepted or rejected following the Metropolis algorithm with the Boltzmann criterion. A single Monte Carlo step (MCS) consists of N (where N is the number of monomers in the chain) attempted moves on randomly picked monomers, effectively setting the time scale.

The thermodynamic collapse transition temperature is $T_\theta(N \rightarrow \infty) \approx 3.7$ in Model I.[6] For Model II there is no study available that quantifies T_θ. We therefore first performed a set of equilibrium simulations and using multiple-histogram reweighting[46,47] obtained an estimate of $T_\theta(4096) \approx 4.0$ for Model II, which is comparatively crude but serves the purpose of indicating the relevant temperature range. For both the models, we prepare well equilibrated initial configurations at high temperatures $T_h = 6 \approx 1.5 T_\theta$ that mimics an extended coil polymer and then quench it to the globular phase at different temperatures $T_q < T_\theta$. We use chains of length N within a wide range $(512 \leq N \leq 8192)$. By using lattice polymers we are thereby able to simulate polymers one order of magnitude longer than in the off-lattice simulations performed in Refs. 21–23.

The time evolution of a single simulation run does depend of course on the randomly chosen initial polymer configuration in the high-temperature extended coil phase. To arrive at meaningful results, the data presented are hence averaged over 300 different initial realizations.

III. NONEQUILIBRIUM DYNAMICS OF THE COLLAPSE TRANSITION

We now continue with the results and analyses of the nonequilibrium dynamics of the collapse. In Figs. 1(a) and 1(b), we show the time evolution snapshots of a polymer quenched to $T_q = 2.5$, for both the models with $N = 8192$. Chronologically, the observed events in both the models are in good accordance with the phenomenological picture of HG.[26] The collapse commences with the formation of nascent-clusters at sites with relatively higher densities along the chain. These clusters subsequently start coarsening by pulling monomers from the chains connecting them and eventually coalesce with each other, forming bigger clusters. This second stage of the collapse finally ends when all the monomers are in a single cluster. Strikingly one can observe in Fig. 1(b) that for Model II the coalescence of clusters not only occurs along the chain but also occurs from the lateral movement of the clusters. One can attribute this to the choice of much larger $N(= 8192)$, which at intermediate times gives rise to structures that resemble branching or a network of "pearls." Thus formation of multiple connections for a cluster to other clusters becomes quite feasible. Although this has not been observed in any previous simulation,[21,23,27] courtesy of using smaller N, one must expect that in the thermodynamic limit $(N \rightarrow \infty)$ this could be the real picture.
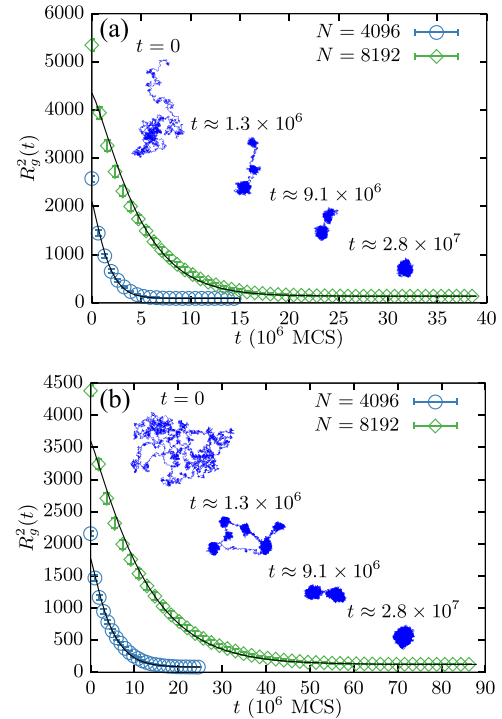

FIG. 1. The decay of the squared radius of gyration for (a) Model I with fixed bonds and (b) Model II with fluctuating bonds at $T_q = 2.5$ for polymers with $N = 4096$ and 8192. The solid black lines show the results of the fit to Eq. (7). Additionally we have included for both models exemplary evolution snapshots of polymer conformations with $N = 8192$.

Next we investigate the scaling of the relaxation time for both the models followed by the study of scaling of cluster coarsening. In the final subsection, we present results related to aging using a suitable two-time correlation function.

A. Relaxation time

Following the general trend used in most of the dynamic studies, we start our analyses with the understanding of the decay of the radius of gyration with time. The squared radius of gyration

$$R_g^2 = \frac{1}{2N^2} \sum_{i,j=1}^{N} (\mathbf{r}_i - \mathbf{r}_j)^2,$$ (6)

where $\mathbf{r}_i$ is the position of i-th monomer, is a measure of the spatial extension or size of a polymer. The plots in Figs. 1(a) and 1(b) show the decay of R_g^2 as a function of time t for Model I and Model II, respectively. For off-lattice models both with[48] and without hydrodynamics,[23] it has been shown that such a decay of R_g^2 can be well described as

$$R_g^2(t) = b_0 + b_1 \exp\left[-(t/\tau_c)^\beta\right],$$ (7)

where b_0 corresponds to the value of R_g^2 in the collapse phase, b_1 and β are two non-trivial fitting parameters, and τ_c is a measure of the relaxation time or the collapse time. In Figs. 1(a) and 1(b), the solid lines are the corresponding best fits to (7), showing more or less a consistent behavior. The fits for all polymer lengths provided a reduced chi-squared value χ_r^2 (χ^2 per degree-of-freedom) close to unity (see Table I) suggesting (7) as an appropriate analytic form. For the estimation of the statistical error on the relaxation times τ_c from (7), we performed a

TABLE I. Results obtained from the Jackknife analysis of fits of the form (7) to the decay of the squared radius of gyration $R_g^2(t)$, for Model I and Model II using three different polymer lengths. The reduced chi-squared χ_r^2 is the average goodness-of-fit parameter.

N	Model	τ_c (10^5 MCS)	β	χ_r^2
2048	I	5.0(3)	1.23(5)	1.5(2)
4096	I	16(1)	1.22(5)	1.5(2)
8192	I	50(3)	1.23(4)	1.7(3)
2048	II	13.3(8)	1.00(5)	0.5(3)
4096	II	46(3)	1.15(5)	1.3(7)
8192	II	126(4)	1.14(4)	2.0(2)

Jackknife analysis[49,50] to mitigate the effect of temporal correlations. We note that the stretching exponent β assumes a constant value of $\beta \approx 1.2$ in Model I, while in Model II we observe a slight variation from $\beta \approx 1.0$ to $\beta \approx 1.15$ for increasing N, similar to the behavior observed in the off-lattice polymer model.[23] One can also estimate the collapse time τ_c by measuring the time t_{50} when $R_g^2(t)$ has decayed to $[R_g^2(0) - R_g^2(\infty)]/2$, i.e., half of its total decay. The collapse times obtained from the fitting of Eq. (7) and as t_{50} are plotted in Figs. 2(a) and 2(b) for Model I and Model II, respectively. Apparently the data show a power-law behavior that one can quantify by using the form

$$\tau_c = BN^z + \tau_0, \tag{8}$$

where B is a nontrivial constant that may depend on the quench temperature T_q, z is the corresponding dynamic critical

exponent, and the offset τ_0 comes from finite-size corrections. In the absence of hydrodynamics, the Rouse model[15] predicts $z = 2$ for such relaxation in equilibrium dynamics. In previous studies of such dynamic exponent in equilibrium dynamics of a lattice polymer with relatively smaller N, a value of $z \approx 2.1$ was reported.[51] The results of fitting the two different collapse times for both models to the form (8) are tabulated in Table II. For Model I (Model II), fitting of the data provides $z \approx 1.73$ ($z \approx 1.62$). These values are somewhat larger but still compatible with the value ($z = 1.5$) predicted in a theory using a coarse-grained picture of the collapsing polymer in the absence of hydrodynamics.[28] Later, we show a possible algebraic connection of z with the cluster-growth exponent α_c.

B. Cluster-growth kinetics

Now, after having an idea on the relaxation times related to the collapse, we shift our focus to the cluster-growth kinetics. The formation and growth of clusters of monomers bear certain resemblance with the coarsening of particle or spin systems.[24,25,52,53] As already mentioned, this fact has been exploited to understand the collapse dynamics in an off-lattice model polymer.[21,23] Following this approach, for the lattice models considered here, the ordered structures (clusters of monomers) can be detected. Thus the formation and growth of clusters can be monitored by measuring the number of clusters N_c and the corresponding size of clusters $C_s(t)$ as a function of time during the collapse. The identification of clusters is achieved by iterating over the polymer and identifying the number of monomers n_i within a distance r_{max} around each monomer i. If this number of monomers n_i exceeds a certain minimum number of monomers ($n_i > n_{min}$), then there is said to be a cluster around monomer i containing all the n_i monomers. The overlap of clusters (a single monomer cannot be part of two or more clusters) introduced by this method is resolved by assigning overlapping clusters into a single cluster. Different combinations of n_{min} and r_{max} produces comparable results in the coarsening regime of cluster growth for reasonable choices. For the results to be presented here we opt for $n_{min} = 10$ and $r_{max} = 2$ as in Ref. 27. Moreover, with the aim of exploiting the advantages of a lattice model to identify ordered structures as well as to characterize the morphology, we calculate a two-point equal-time density-density correlation function, defined as

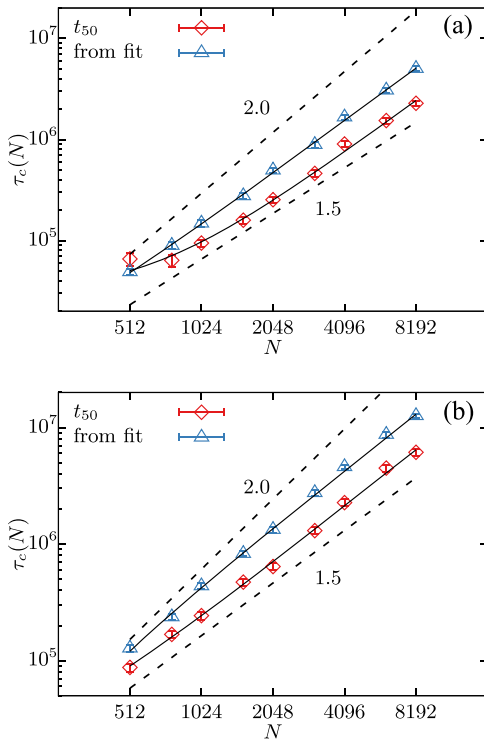$$C(r,t) = \langle \rho_i(0,t)\rho_i(r,t) \rangle, \tag{9}$$

FIG. 2. Double-log plots showing the scaling of the relaxation time τ_c obtained from two different methods for (a) Model I and (b) Model II at $T_q = 2.5$. The solid lines are the best fits of (8), with parameters as mentioned in Table II. The dashed lines represent the Rouse behavior $\tau_c \sim N^2$, respectively, the theoretical prediction $\tau_c \sim N^{1.5}$ of Ref. 28.

TABLE II. Results obtained from the fits of (8) to the relaxation times τ_c for the full range of data $N \in [512, 8192]$, using both the models. Here again χ_r^2 measures the goodness of fit.

Method	Model	Z	χ_r^2
t_{50}	I	1.72(8)	1.61
From fit	I	1.73(5)	0.56
t_{50}	II	1.61(5)	1.08
From fit	II	1.62(4)	1.50

where

$$\rho_i(r,t) = \frac{1}{m_r} \sum_{j, r_{ij}=r} \theta(\mathbf{r}_j, t). \tag{10}$$

The characteristic function θ is unity if there is a monomer at a position $\mathbf{r}_j$ or zero otherwise. The number of possible lattice points at distance r from an arbitrary point of the lattice is denoted by m_r, which obviously is dependent on the type of underlying lattice.

In Fig. 3(a) we plot such exemplary $C(r,t)$ at four different times for Model II quenched to $T_q = 2.5$. The signature of the presence of a growing nonequilibrium length scale is clearly evident as the curves decay farther with the increase in time. For Model I and different quench temperatures T_q we observe similar behavior; however, we do not present such plots for the sake of brevity. Following the exercise prevailed in phase-ordering business,[24,25] we extract an average length scale $\ell(t)$ that describes the ordering, i.e., clustering during the collapse, using the criterion

$$C[r = \ell(t), t] = h, \tag{11}$$

where we chose $h = 0.1$. Other values of h produce a proportional behavior. For the characteristic length $\ell(t)$, following the trend in ordering phenomena studies, one looks for the scaling of the form

$$C(r,t) \equiv \tilde{C}(r/\ell(t)), \tag{12}$$

where $\tilde{C}$ is the scaling function. The presence of such scaling is demonstrated in Fig. 3(b), showing the collapse of $C(r,t)$ for Model II at different times when plotted as function of $r/\ell(t)$.

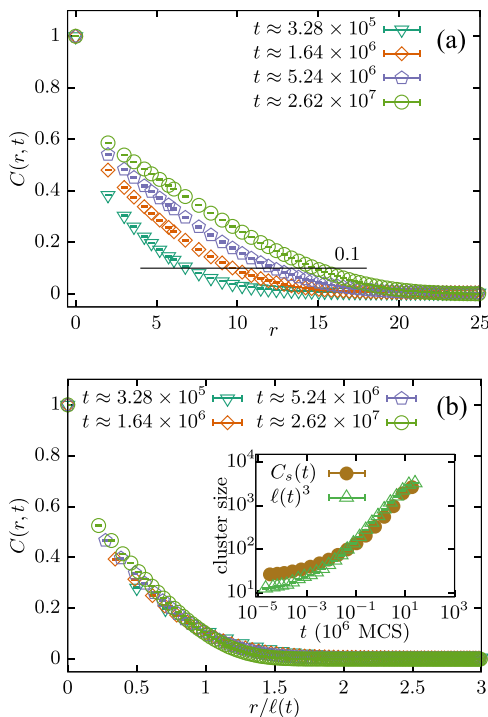

FIG. 3. (a) Two-point equal-time correlation function $C(r,t)$, at different times for Model II. The solid line depicts the extraction of the characteristic length $\ell(t)$ using $h = 0.1$ in (11). (b) The corresponding scaling plots as a function of $r/\ell(t)$. The inset of (b) shows the comparison of $\ell(t)^3$ and the cluster size $C_s(t)$ on a log-log scale. All the results are obtained for $N = 4096$ monomers for a quench at $T_q = 2.5$. The time t is denoted in units of Monte Carlo sweeps (MCS).

Although we do not present it here, Model I shows a similarly good scaling.

Since the ordering during collapse is manifested by the formation of the clusters of monomers, the characteristic length $\ell(t)$ must be related to the cluster size $C_s(t)$, obtained via the cluster recognition method such that

$$C_s(t) \propto \ell(t)^{d_f}, \tag{13}$$

where d_f is the fractal dimension of the clusters. To estimate this fractal dimension, we set the radius of gyration for each single cluster in relation to its mass (number of monomers) and obtain $d_f \approx 3$. In the inset of Fig. 3(b) we compare $\ell(t)^3$ with $C_s(t)$ for Model II at quench temperature $T_q = 2.5$. Apart from a little discrepancy at early times they seem to be proportional to each other. Based on this observation, hence, from now onward, we will use $\ell(t)^3$ to characterize the cluster growth. In particular this has advantages at comparatively higher quench temperatures T_q, where the cluster identification method fails to recognize the final globular structure as a single cluster for a single chosen set of n_{min} and r_{max}.

Now, from the scaling of $C(r,t)$ one can easily deduce the fact that the ordering or rather the cluster growth follows a power-law scaling $\ell(t)^3 \sim t^{\alpha_c}$. As already mentioned,[21,23] due to the involvement of crossover from the initial cluster formation stage, the true scaling behavior is described by (1). We start our quantification by replacing $C_s(t)$ with $\ell(t)^3$, where $\ell(t)$ is extracted using (11), in (1) to obtain

$$\ell(t)^3 = \ell_0^3 + A t^{\alpha_c}. \tag{14}$$

Figure 4 shows the time dependence of $\ell(t)^3$ for different polymer lengths, as indicated, with the same data shown for only $N = 8192$ on a double-log scale in the inset, for (a) Model I and (b) Model II. The data for different N follow each other until finite-size effects become apparent. The finite-size effect creeps in when all the monomers become part of a single cluster, and thereby no further growth is observed. Initially there is a transition period in the growth (can be seen from the double-log scale plot), marking the initial stage of cluster formation. After the initial clusters are formed, the growth crosses over to the coarsening regime where it indeed shows a power-law scaling. The data in both cases seem to have a higher slope than the solid lines with exponent 1/2, as observed in Ref. 27. We use the form (14) to fit the data, considering the crossover in the growth. This yields

$$\alpha_c = 0.68(6) \text{ for Model I}$$

and

$$\alpha_c = 0.62(5) \text{ for Model II}.$$

1. Temperature-dependence of the cluster growth

Next we turn to a check of the robustness of the kinetics for both the models, viz., the influence of the quench temperature T_q. In simulations of various off-lattice models, it has been shown that changing temperature correctly reproduces the change in solvent quality, with faster collapse as the temperature decreases.[23,48] In contrast, here we find that a decrease in temperature results in a slower collapse, similar to the behavior observed for ordering dynamics of the
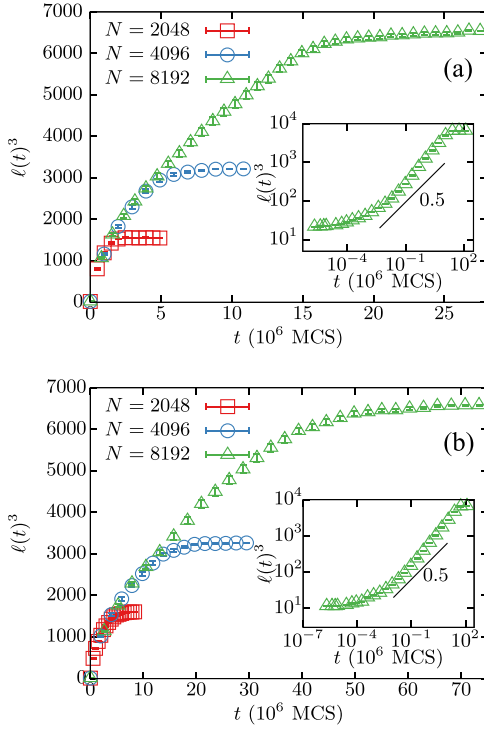
FIG. 4. Plot of the cubed characteristic length $\ell(t)^3$, as a measure of the average cluster size, against time for (a) Model I and (b) Model II with N = 2048, 4096, and 8192 quenched to T_q = 2.5. The insets show the data for N = 8192 on a double-log scale. The solid lines there show power-law behaviors with exponent 1/2.

FIG. 5. Double-log plot showing the dependence of the cluster growth on the quench temperature T_q in (a) Model I and (b) Model II, measured as $\ell(t)^3$ for N = 4096. The inset shows the respective time-dependent instantaneous exponent $\alpha_c(t)$ calculated as described in Eq. (15).

Ising model,[54] where faster equilibration occurs at higher temperature due to increasing diffusion of particles. In addition, for low enough temperatures, the system may get trapped in some metastable state with high energy barrier, quite difficult to overcome via simple Metropolis dynamics. Thus to avoid such situations, we restrict ourselves to simulations at relatively higher temperatures $T_q \in [2.0, 2.75]$.

We show the growth of clusters for Model I at different T_q in the main frame of Fig. 5(a). It is apparent that, within the chosen range of temperature, the scaling of the growth is non-universal in nature. On the other hand, for Model II, shown in the main frame of Fig. 5(b) the growth looks quite independent of T_q. A fitting with the form (14) provides α_c having a wide range [0.5, 0.8] for Model I whereas for Model II a much narrower range [0.58, 0.65] is obtained. In this regard, we also calculate the instantaneous exponent $\alpha_c(t)$ given as

$$\alpha_c(t) = \frac{d \ln \ell(t)^3}{d \ln t}, \quad (15)$$

which when operated on (14) yields

$$\alpha_c(t) = \alpha_c \left[1 - \frac{\ell_0^3}{\ell(t)^3} \right]. \quad (16)$$

Thus a plot of $\alpha_c(t)$ against $1/\ell(t)^3$ would provide the asymptotic α_c in the limit $1/\ell(t)^3 \to 0$. In the insets of Figs. 5(a) and 5(b) we show such plots of $\alpha_c(t)$ for the respective models. The asymptotic behavior clearly indicates that the growth in Model II is of more universal nature. Like in Model I, temperature-dependent growth exponents were earlier observed in quenches of an Edwards-Anderson spin glass
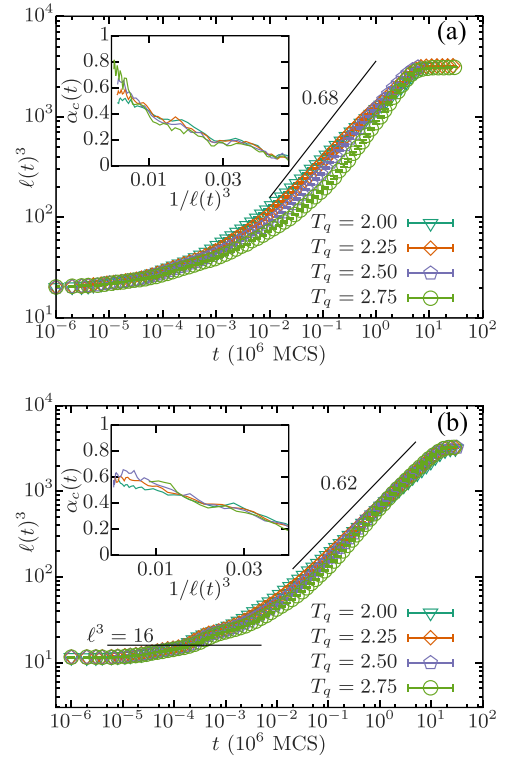
in $d = 3$,[55] in an anisotropic rotor model with vacancies[56] as well as in disordered ferromagnets.[57–59] This connection might be reasonable, as all the concerned systems are dominated by disorder and constraints of the lattice structure. On the other hand, perhaps the introduction of bond fluctuation due to consideration of the diagonal bonds helps to overcome the topological constraints of the lattice to some extent, hence, a temperature-independent growth at moderately high temperatures.

For both models the growth exponent is smaller than in the off-lattice model where $\alpha_c \approx 1$.[21,23] For Model I, however, the value of α_c is not universal, as the growth exponent appears to be dependent on the quench temperature T_q. The value obtained for Model II already gives an indication for a different (temperature-independent) growth exponent than 1/2 as reported in Ref. 27. For further investigation we call for a nonequilibrium finite-size scaling analysis for Model II.

2. Finite-size scaling analysis

Using a finite-size scaling analysis one aims at extracting quantities in the thermodynamic limit ($N \to \infty$) from simulations of a finite size. In simulations we necessarily have finite systems and thus this analysis method has its wide application in the context of critical phenomena.[60] Later finite-size scaling has also been successfully adapted to the nonequilibrium scenario to understand the growth exponents in particle[61] and spin[52,53] systems. Here, we rely on such an exercise previously performed in more detail for the off-lattice model in Ref. 23. This method was applied successfully to understand the collapse dynamics. The finite-size scaling ansatz is

constructed by generalizing Eq. (14) to additionally include an initial crossover time t_0,

$$\ell(t)^3 = \ell_0^3 + A(t - t_0)^{\alpha_c}. \qquad (17)$$

The values of ℓ_0 and t_0 are marking the point after which the coarsening regime starts and are analogous to the background contribution in critical phenomena. Following Ref. 23, we identify the linear cluster size $\ell(t)$ ($\sim C_s(t)^{1/3}$) with the equilibrium correlation length ξ, and $1/t$ with the temperature deviation from a critical point. In order to account for the finite-size effect in (17), one can write down[23]

$$\ell(t)^3 - \ell_0^3 = (\ell_{\max} - \ell_0)Y(y), \qquad (18)$$

with the finite-size scaling function

$$Y(y) = \frac{\ell(t)^3 - \ell_0^3}{\ell_{\max}^3 - \ell_0^3} \qquad (19)$$

and the scaling variable

$$y = \frac{(\ell_{\max}^3 - \ell_0^3)^{\frac{1}{\alpha_c}}}{t - t_0}. \qquad (20)$$

Note that in (18)–(20) $\ell_{\max}$ is the saturation value of $\ell(t)$, which one obtains when all the monomers of the polymer are in a single dense globular cluster, and does not need to be equal to $N^{1/3}$, but rather proportional, $\ell_{\max} \sim N^{1/3}$. In the finite-size unaffected regime, the form (17) is recovered, providing

$$Y(y) \propto y^{-\alpha_c}, \qquad (21)$$

while in the finite-size affected regime one must obtain $Y(y) \to 1$. In the finite-size scaling exercise, we tune the value of α_c to obtain an optimum collapse of data for different N, obeying the master curve behavior (21). From the fitting exercise done in Sec. III B 1, we have a fair idea about ℓ_0. We chose $\ell_0^3 \approx 16$ and $t_0 \approx 200$ for Model II, independent of N. The exercise yields a reasonably good collapse of data and corresponding master curve behavior with $\alpha_c = 0.62(3)$ for Model II, in agreement with the direct fit. In Fig. 6 we present a representative plot for Model II. The corresponding plot for Model I is omitted due to the quench-temperature dependency. On one hand, the value obtained is different from the previously reported value of 1/2 for a lattice polymer.[27] On the other hand $\alpha_c \approx 2/3$ is comparable with the value predicted for an

off-lattice model via Gaussian self-consistent theory,[31] confirmed by Langevin dynamic simulations.[30] On the contrary, for a similar off-lattice model, however, one observes a linear cluster growth[21,23] as observed for Ostwald ripening (corresponding to the Ostwald exponent 1/3 when considering the length scale). Now, by using the fact that at the point of onset of finite-size effects $\ell(t)^3 \sim N$ and by replacing the corresponding time t as the collapse time τ_c, one can show[23] from (19) and (20) that $z = 1/\alpha_c$. This relation holds quite nicely for Model II as it yields $z \approx 1.61$, consistent with the behavior shown in Fig. 2 and Table II.

3. Temperature-dependent scaling of the cluster growth

To further look into the universal nature of the scaling in Model II, we apply a modified scaling analysis based on the above discussed finite-size scaling analysis. Here we account for the different growth amplitudes by modifying the scaling variable (20) as[23]

$$y_p = f_s \frac{(\ell_{\max}^3 - \ell_0^3)^{\frac{1}{\alpha_c}}}{t - t_0}, \qquad (22)$$

with a metric factor depending on the growth amplitudes,

$$f_s(T_q) = \left(\frac{A(T_q = 2.0)}{A(T_q)} \right)^{\frac{1}{\alpha_c}}. \qquad (23)$$

Note that y_p differs from y only by this factor f_s. A fitting of the $\alpha_c(t)$ presented in the inset of Fig. 5(b) to the scaling law (16) provides a rough estimate of $\ell_0^3 = 16 \pm 2$ for all quench temperatures, consistent with the previously mentioned value of $\ell_0^3 \approx 16$ for the polymer quenched to $T_q = 2.5$. We use this value of ℓ_0^3 and the corresponding t_0 values in the scaling exercise and tune the value of α_c such that the data for different T_q collapse onto a single master curve for appropriate adjustments of the metric factor f_s, i.e., the ratio of amplitudes. Recall that an appropriate choice of α_c should lead to a consistent power-law behavior of the finite-size scaling function as $Y(y_p) \sim y_p^{-\alpha_c}$ along with optimum data collapse. In our exercise we obtained such behavior for $\alpha_c = 0.62(4)$. In Fig. 7, we show such a representative plot for $\alpha_c = 0.62$. The successful application of such a scaling exercise thus indicates that indeed the scaling of cluster growth in the Model II is nearly universal in nature which can be described by a universal finite-size scaling function with a non-universal metric factor. This observation has
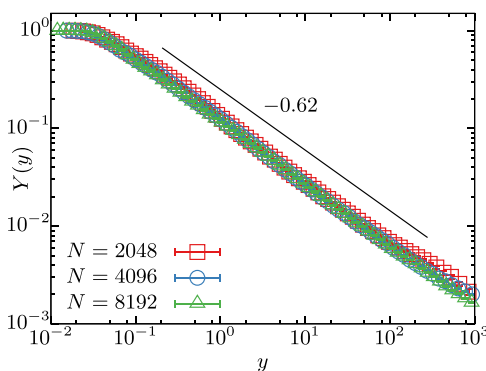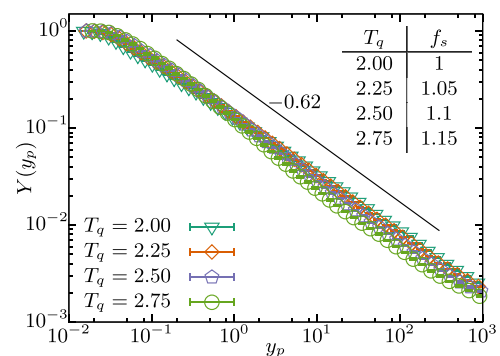

FIG. 6. Finite-size scaling plot for Model II at $T_q = 2.5$ using the ansatz (17). The solid line corresponds to the expected power-law decay with an exponent $\alpha_c = 0.62$.

FIG. 7. Scaling plot for Model II for different quench temperatures T_q, where f_s is the metric factor defined in Eq. (23). The solid line corresponds to a power-law function with exponent $\alpha_c = 0.62$.

recently been made in an off-lattice model,[21,23] however, for a linear scaling of the cluster growth.

C. Aging and related scaling

Until now, our focus has been solely on equal-time quantities governing the kinetics. Here, in this subsection we turn our attention to the behavior of a two-time quantity, used to probe aging in an evolving nonequilibrium system. Using the framework recently developed for an off-lattice model,[22,23,62] we construct the two-time correlation function as

$$C(t, t_w) = \langle O_i(t)O_i(t_w) \rangle - \langle O_i(t) \rangle \langle O_i(t_w) \rangle. \quad (24)$$

We assign $O_i = \pm 1$ by checking the radius r, at which the local density, given by $\rho_i(r, t)$ [see Eqs. (9) and (10)], first falls below a threshold of 0.1. If this radius is smaller than $\sqrt{3}$, we assign $O_i = 1$, marking a high local density, otherwise we chose $O_i = -1$ to mark a low local density. This definition is an adaptation of the method used in Refs. 22 and 23, where one relies on the cluster identification method. Nonetheless, both methods are analogous to the usual two-time density-density correlation function in particle systems. In Fig. 8(a), $C(t, t_w)$ is plotted against the translated time $t - t_w$ at different values of the waiting time t_w for Model I and in (b) for Model II with a polymer of length $N = 8192$, quenched to $T_q = 1.5$. Note here that the quench temperature T_q is lower than in Sec. III B. It will become clear as we move forward that here the scaling is independent of T_q for both the models. One can clearly see that the data for different t_w do not overlap and the decay becomes slower with increasing waiting time t_w. Such an absence of time-translation invariance is a necessary condition for aging

in the system. In case of simple aging as described by (2), assuming an algebraic growth of the relevant length scale, one expects

$$C(t, t_w) \equiv g(t/t_w), \quad (25)$$

where g is the scaling function of the variable t/t_w. While plotting $C(t, t_w)$ as a function of t/t_w we fail to observe any scaling for both the models as shown in Fig. 9(a) for Model I and Fig. 9(b) for Model II.

Such observation of "no data collapse" is known in ordering kinetics of diluted ferromagnets.[59,63] This led the authors of Ref. 59 to use a special fitting ansatz given as

$$C(t, t_w) \equiv G\left(\frac{h(t)}{h(t_w)}\right), \quad (26)$$

with the argument

$$h(t) = \exp\left(\frac{t^{1-\mu} - 1}{1 - \mu}\right). \quad (27)$$

Here, G is the scaling function and μ is a nontrivial exponent. Such an exercise with $\mu > 1$ indeed provided them an apparently reasonable collapse of the data. This is referred to as the so-called superaging behavior. However, it is known that algebraic constraints on the form of the autocorrelation function rule out the existence of such superaging behavior.[64] Later, while the analysis of Ref. 63 numerically convincingly suggested that such an ansatz may indeed be a good fitting function that provides a reasonable collapse of data, the true scaling behavior has been shown by these authors to be realized when one instead uses the generic scaling form (2).

Observation of data collapse using (26) with $0 < \mu < 1$ is referred to as subaging, observed mostly in soft matter systems.[65] Previously this has also been observed for a collapsing polymer.[66,67] We have tested the scaling ansatz of Eqs. (26) and (27) with our data and tuned the exponent μ by trial and error until best data collapse is realized. We find $\mu \approx 0.9$ for both models. The corresponding scaling plots are shown in Fig. 9(c) for Model I and (d) for Model II. However, when we now simply plot $C(t, t_w)$ as a function of the ratio of cluster sizes $x_c = \ell(t)^3/\ell(t_w)^3$, as shown in Figs. 9(e) and 9(f) for both the models, we also observe a reasonable collapse of data.[68] This implies that, in the present case, too, the generic form (2) describes the true scaling behavior rather than any special aging.

In Ref. 63, it has been argued that the simple aging of the form (25) has been deduced considering an algebraic growth of the relevant length scale. However, in their case a crossover from the algebraic growth to a slower logarithmic growth in the asymptotic limit makes such deduction meaningless, hence, the absence of simple scaling with respect to t/t_w. In the present case, for clustering during the polymer collapse also, we encountered a crossover from a transient period of growth in the initial cluster formation stage to a faster growth in the coarsening or coalescence stage, a fact that can be appreciated from the insets shown in Fig. 4. This reversal of crossover in our case could be the reason for the apparent appearance of subaging behavior with $\mu < 1$, in contrast to the superaging behavior, where the crossover occurs the other way around.

Our next task is to have a measure of the dynamic exponent λ_C governing the scaling (2). In Figs. 9(e) and 9(f), the scaling
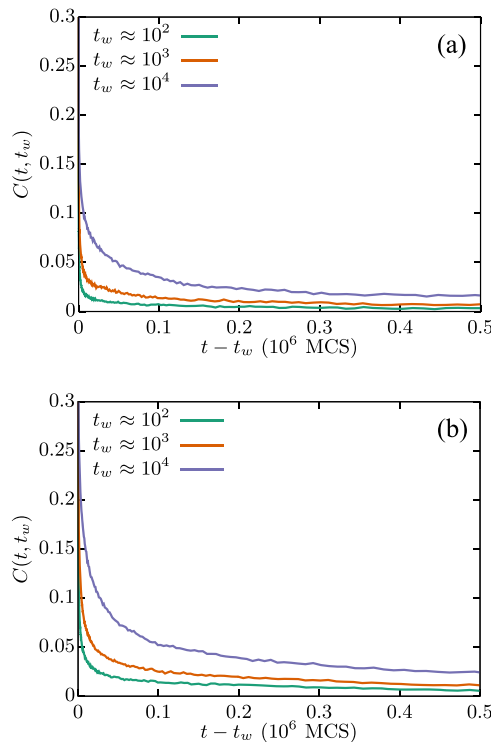

FIG. 8. Plot of two-time correlation functions $C(t, t_w)$ against $t - t_w$ for (a) Model I and for (b) Model II. The exact values of t_w are very close to the indicated value. The length of the polymer used here is $N = 8192$ and the corresponding quench temperature is $T_q = 1.5$.
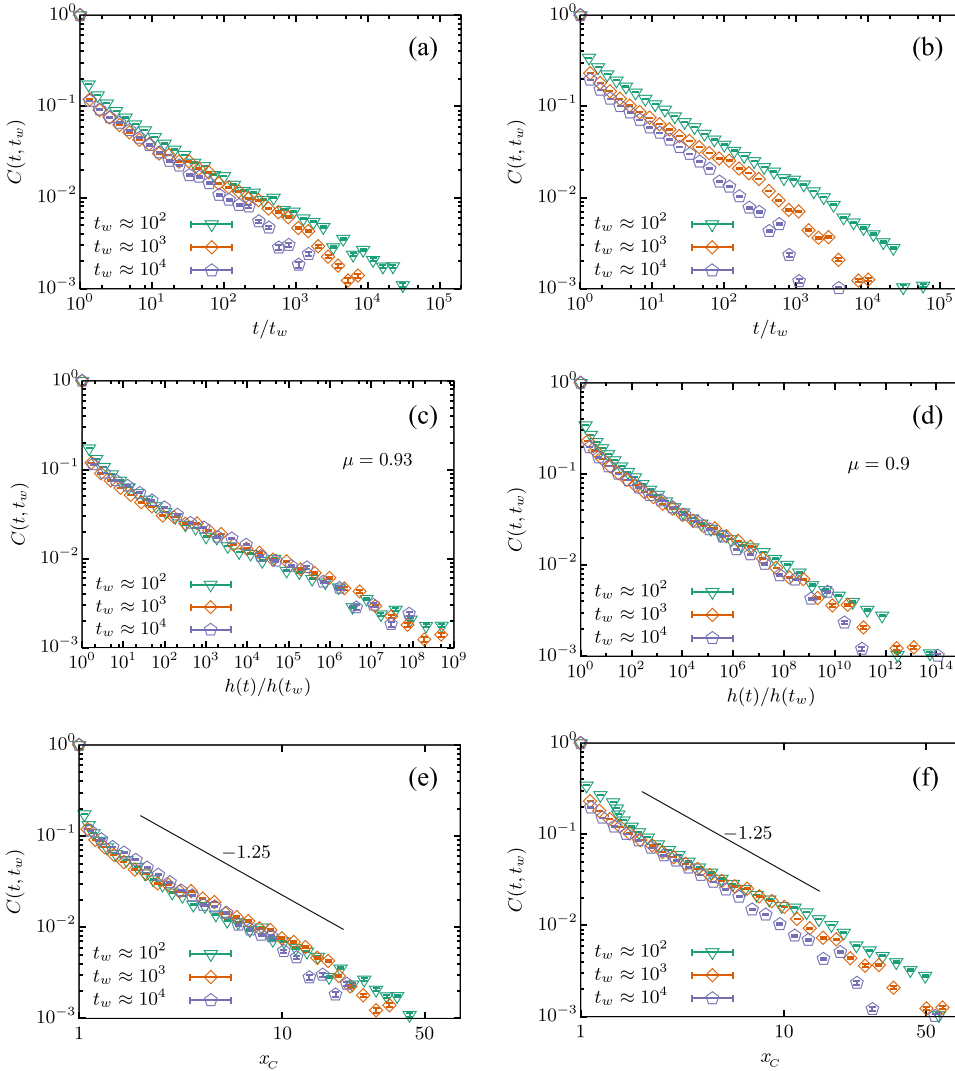
FIG. 9. The scaling of the two-time correlation function $C(t, t_w)$ with respect to t/t_w is shown in (a) for Model I and (b) for Model II. The scaling of form (26) is shown in (c) for Model I and (d) for Model II. The value of μ was obtained by trial and error to get the best data collapse. In (e) for Model I and (f) for Model II, the scaling with respect to the ratio of the cluster sizes, i.e., $x_C = \ell(t)^3/\ell(t_w)^3$ is presented. The solid lines in those plots show a power-law decay with slope -1.25. In all plots of this figure, the same data are presented, as can be seen from the range of values for the two-time correlation function $C(t, t_w)$. The length of the polymer used here is $N = 8192$ and the corresponding quench temperature is $T_q = 1.5$.

plots show that the data for $x_c \gg 1$ are consistent with the continuous line having slope -1.25. In this regard, when the numerically precise value[69] of ν is inserted in the bound (3) for λ_C, one gets

$$0.762\,791 \leq \lambda_C \leq 1.525\,582. \tag{28}$$

The obtained $\lambda_C = 1.25$ from Figs. 9(e) and 9(f) for both Model I and Model II thus not only follows the general theoretically bound (3) but also seems to be in agreement with the numerical estimates obtained for the off-lattice model in Refs. 22, 23, and 62.

1. Finite-size scaling analysis

To further substantiate the numerical estimate of λ_C, we call for a finite-size scaling analysis using data for three different system sizes shown in Figs. 10(a) and 10(b), respectively, for Model I and Model II. Note that here we have used a fixed t_w ($=10^3$ MCS), hence the onset of finite-size effects (the downward tendency of the data) occurs earlier for smaller N. We do a finite-size scaling analysis based on the scaling form (2) by writing down our finite-size scaling ansatz as

$$NC(t, t_w) = Y_a(y_a), \tag{29}$$

where for the judicial choice of the scaling variable

$$y_a = x_c(NA_C)^{-1/\lambda_C}, \tag{30}$$

one gets $Y_a \sim y_a^{-\lambda_C}$, i.e., $y_a \sim Y_a^{-1/\lambda_C}$. In our exercise, we fix $A_C = 1$ and by varying λ_C obtain reasonable data collapse for $\lambda_C = 1.25(5)$, consistent with the obtained value for different waiting times t_w. In Figs. 11(a) and 11(b), we show the representative plots for the finite-size scaling exercise for Model I and Model II, respectively, with $\lambda_C = 1.25$. Both the models show reasonable quality of collapse of data and consistent behavior with $y_a \sim Y_a^{-1/\lambda_C}$. Note that here the crossover to the finite-size affected limit for smaller values of Y_a from the scaling regime occurs rather gradually in contrast to the corresponding picture in an off-lattice model.[22]

2. Temperature-dependent scaling of aging

This universal nature of λ_C, irrespective of the details of models, thus urges us to check its robustness in the present models at different quench temperatures, especially considering our observation of a rather non-universal nature of the other dynamic exponent α_c for Model I. In Fig. 12, we show for the chain of length $N = 4096$ the temperature effect on the behavior of the autocorrelations $C(t, t_w)$ as a function of x_c for fixed waiting time $t_w = 10^3$. There the y–axis has to be multiplied by
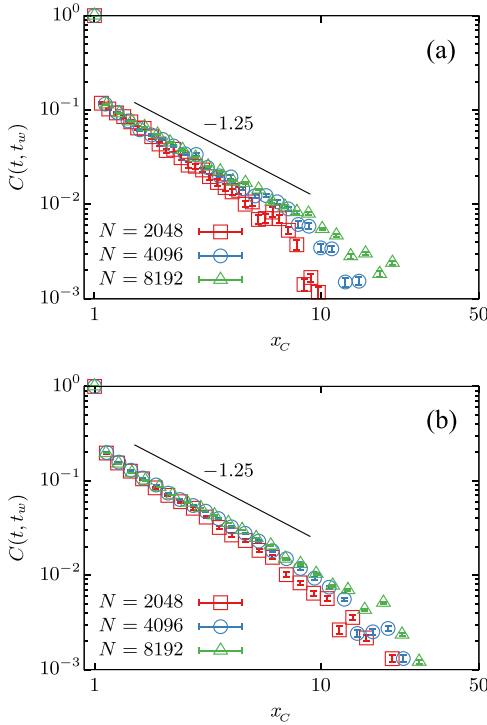
FIG. 10. $C(t, t_w)$ for $N = 2048$, 4096, and 8192 for (a) Model I and (b) Model II quenched to $T_q = 1.5$ with $t_w = 10^3$ fixed against $x_C = \ell(t)^3/\ell(t_w)^3$.

a factor $f = A_C(T_q = 1)/A_C(T_q)$, similar to the metric factors in Fig. 7, to make them collapse onto a single master curve. This master-curve behavior at different T_q implies that, in contrast
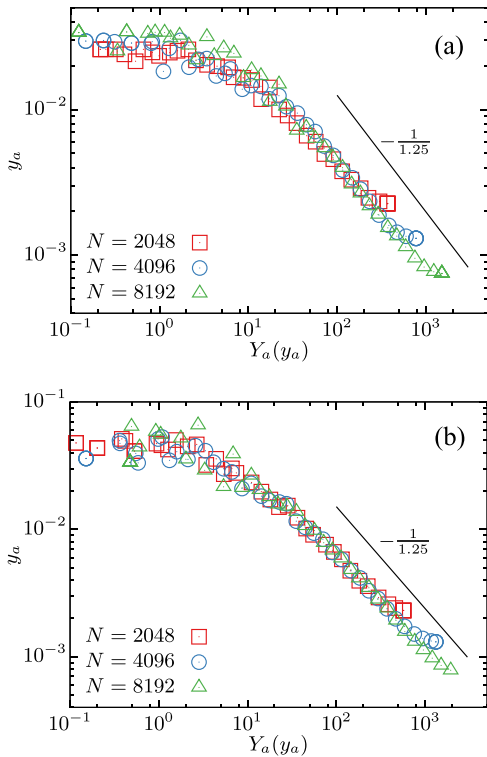

FIG. 11. Finite-size scaling plot of $C(t, t_w)$ for $N = 2048$, 4096, and 8192 for quench temperature $T_q = 1.5$ with $t_w = 10^3$ fixed for (a) Model I and (b) Model II. The scaling behavior $y_a \sim Y_a^{-1/\lambda_C}$ is reasonably well observed for $\lambda_C = 1.25$.
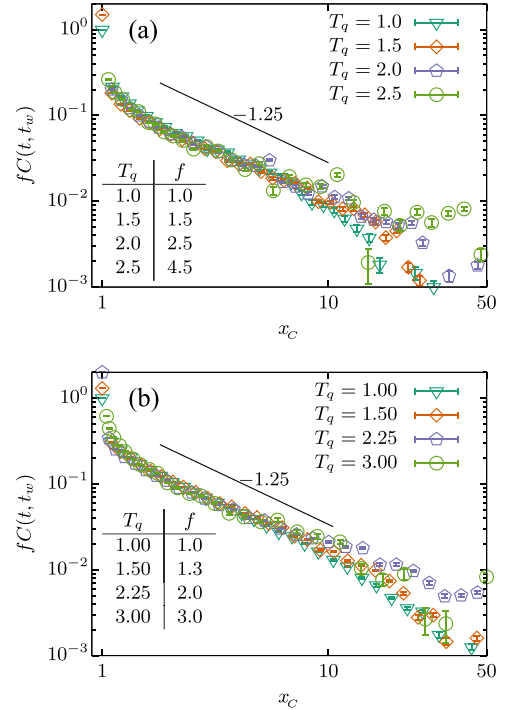

FIG. 12. Plots to show the scaling of $C(t, t_w)$ with respect to $x_C = \ell(t)^3/\ell(t_w)^3$ at different quench temperatures T_q for (a) the fixed bond Model I and (b) the fluctuating bond Model II with $N = 4096$, for fixed $t_w \approx 10^3$. To obtain the data collapse, the two-time correlation functions were multiplied by a growth amplitude dependent factor f, whose values are quoted in the figure.

to the cluster growth exponent, both models are found to be following the same power-law decay of the autocorrelations at different T_q. This further strengthens the dynamic universal behavior of the aging exponent λ_C concerning the collapse of a polymer.

IV. CONCLUSION

We have presented results from the kinetics of collapse for a lattice homopolymer in dimension $d = 3$ using two different bond types, that is, with fixed and fluctuating bonds. The cluster growth that occurs during the collapse is a scaling phenomenon as observed from the scaling of the two-point equal-time correlation function. However, for Model I with fixed bonds, the growth of the clusters appears to be strongly dependent on the quench temperature. Similar observations were observed for ordering phenomena in disordered magnets.[55–59] On the other hand, Model II where the bonds have the flexibility of switching lengths between edges and diagonals of the lattice produces a much weaker dependence of the growth on the quench temperature. In fact, for moderately high temperatures, we show that the cluster growth can be described by an universal finite-size scaling function, pretty much like an off-lattice model. The growth exponent $\alpha_c \approx 0.62$ that we have estimated for such a description, however, is much smaller than what was observed for the off-lattice model[21,23] that exhibits a linear growth. This we feel is attributed to the topological constraint one encounters in a lattice model, a fact, though expected, needs still to be verified. In this regard, it would be worth investigating the kinetics in the bond-fluctuation model.[16] In equilibrium it has been shown that it produces the

correct dynamical picture and one must expect that the topological constraints can be overcome more easily, which may lead to a much more universal picture of the cluster growth.

Regarding the other aspect of the kinetics of collapse, i.e., aging, both the models produced a rather universal picture independent of quench temperature. Although the absence of scaling for the autocorrelation function with respect to t/t_w suggested the presence of subaging, we have shown that the simple aging behavior is realized when one observes the scaling with respect to the ratio of growing cluster sizes, i.e., $C(t, t_w) \sim [\ell(t)^3/\ell(t_w)^3]^{-\lambda_C}$. We also show that the nonequilibrium autocorrelation exponent λ_C, governing such scaling is independent of the model as well as the quench temperature, and the observed value of $\lambda_C = 1.25(5)$ not only follows the general bound $(\nu d - 1) \leq \lambda_C \leq 2(\nu d - 1)$ but also matches perfectly with the corresponding exponent from an off-lattice simulation.[22,23,62] For ordering ferromagnets in dimension $d = 2$, the nonequilibrium order-parameter autocorrelation exponent has been found to be $\lambda_C \simeq 5/4$,[35–41] matching with the value found in our present study for polymer collapse in lattice models and in Refs. 22 and 23 for a continuum formulation, both in $d = 3$ dimensions. Due to the dimensional differences between the systems, we feel that this could be a mere coincidence and further investigation is required to confirm any true non-trivial relationship.

To conclude, we have shown how the methodologies popular in studies of ordering dynamics of particle and spin models can well be used to understand the kinetics of polymer collapse. Hence, we strongly believe that by using a similar framework one could provide new insights into the mechanisms of other macromolecular conformational transitions such as collapse or folding of proteins or peptides using the hydrophobic-polar (HP) model.[44,70] Furthermore, it would also be interesting to check the validity of the various scaling laws discussed here for bulk polymers in lower dimension $d = 2$ and for proteins in quasi-two-dimensional geometry, e.g., for macromolecules adsorbed on a substrate.

ACKNOWLEDGMENTS

[1]D. P. Landau and K. Binder, *A Guide to Monte Carlo Simulations in Statistical Physics* (Cambridge University Press, Cambridge, 2014).
[2]C. Appert and S. Zaleski, "Lattice gas with a liquid-gas transition," Phys. Rev. Lett. **64**, 1 (1990).
[3]R. J. Baxter, *Exactly Solved Models in Statistical Mechanics* (Elsevier, Amsterdam, 1982).
[4]P. Grassberger and R. Hegger, "Simulations of three-dimensional θ polymers," J. Chem. Phys. **102**, 6881 (1995).
[5]P. Grassberger, "Pruned-enriched Rosenbluth method: Simulations of θ polymers of chain length up to 1 000 000," Phys. Rev. E **56**, 3682 (1997).
[6]T. Vogel, M. Bachmann, and W. Janke, "Freezing and collapse of flexible polymers on regular lattices in three dimensions," Phys. Rev. E **76**, 061803 (2007).
[7]W. H. Stockmayer, "Problems of the statistical thermodynamics of dilute polymer solutions," Makromol. Chem. **35**, 54 (1960).
[8]I. Nishio, S.-T. Sun, G. Swislow, and T. Tanaka, "First observation of the coil–globule transition in a single polymer chain," Nature **281**, 208 (1979).
[9]C. J. Camacho and D. Thirumalai, "Kinetics and thermodynamics of folding in model proteins," Proc. Natl. Acad. Sci. U. S. A. **90**, 6369 (1993).
[10]G. Haran, "How, when and why proteins collapse: The relation to folding," Curr. Opin. Struct. Biol. **22**, 14 (2012).
[11]C. Domb, "Self-avoiding walks on lattices," in *Advances in Chemical Physics* (John Wiley & Sons, Hoboken, 2007), pp. 229–259.
[12]P. J. Flory, *Principles of Polymer Chemistry* (Cornell University Press, Ithaca, 1953).
[13]F. Rampf, W. Paul, and K. Binder, "On the first-order collapse transition of a three-dimensional, flexible homopolymer chain model," Europhys. Lett. **70**, 628 (2005).
[14]P. H. Verdier and W. H. Stockmayer, "Monte Carlo calculations on the dynamics of polymers in dilute solution," J. Chem. Phys. **36**, 227 (1962).
[15]P. E. Rouse, Jr., "A theory of the linear viscoelastic properties of dilute solutions of coiling polymers," J. Chem. Phys. **21**, 1272 (1953).
[16]I. Carmesin and K. Kremer, "The bond fluctuation method: A new effective algorithm for the dynamics of polymers in all spatial dimensions," Macromolecules **21**, 2819 (1988).
[17]J. S. Shaffer, "Effects of chain topology on polymer dynamics: Bulk melts," J. Chem. Phys. **101**, 4205 (1994).
[18]T. Dotera and A. Hatano, "The diagonal bond method: A new lattice polymer model for simulation study of block copolymers," J. Chem. Phys. **105**, 8413 (1996).
[19]J. Tang, N. Du, and P. S. Doyle, "Compression and self-entanglement of single DNA molecules under uniform electric field," Proc. Natl. Acad. Sci. U. S. A **108**, 16153 (2011).
[20]M. Tress, E. U. Mapesa, W. Kossack, W. K. Kipnusu, M. Reiche, and F. Kremer, "Glassy dynamics in condensed isolated polymer chains," Science **341**, 1371 (2013).
[21]S. Majumder and W. Janke, "Cluster coarsening during polymer collapse: Finite-size scaling analysis," Europhys. Lett. **110**, 58001 (2015).
[22]S. Majumder and W. Janke, "Evidence of aging and dynamic scaling in the collapse of a polymer," Phys. Rev. E **93**, 032506 (2016).
[23]S. Majumder, J. Zierenberg, and W. Janke, "Kinetics of polymer collapse: Effect of temperature on cluster growth and aging," Soft Matter **13**, 1276 (2017).
[24]A. J. Bray, "Theory of phase-ordering kinetics," Adv. Phys. **51**, 481 (2002).
[25]*Kinetics of Phase Transitions*, edited by S. Puri and S. Wadhawan (CRC Press, Boca Raton, 2009).
[26]A. Halperin and P. M. Goldbart, "Early stages of homopolymer collapse," Phys. Rev. E **61**, 565 (2000).
[27]Y. A. Kuznetsov, E. G. Timoshenko, and K. A. Dawson, "Kinetics at the collapse transition of homopolymers and random copolymers," J. Chem. Phys. **103**, 4807 (1995).
[28]C. F. Abrams, N.-K. Lee, and S. P. Obukhov, "Collapse dynamics of a polymer chain: Theory and simulation," Europhys. Lett. **59**, 391 (2002).
[29]N. Kikuchi, J. F. Ryder, C. M. Pooley, and J. M. Yeomans, "Kinetics of the polymer collapse transition: The role of hydrodynamics," Phys. Rev. E **71**, 061804 (2005).
[30]A. Byrne, P. Kiernan, D. Green, and K. A. Dawson, "Kinetics of homopolymer collapse," J. Chem. Phys. **102**, 573 (1995).
[31]Y. A. Kuznetsov, E. Timoshenko, and K. A. Dawson, "Kinetic laws at the collapse transition of a homopolymer," J. Chem. Phys. **104**, 3338 (1996).
[32]This corresponds to the familiar value of the Ostwald ripening exponent 1/3 obtained when considering the linear size of ordered structures.
[33]M. Zannetti, "Aging in domain growth," in *Kinetics of Phase Transitions*, edited by S. Puri and S. Wadhawan (CRC Press, Boca Raton, 2009), pp. 153–202.
[34]M. Henkel and M. Pleimling, *Non-Equilibrium Phase Transitions, Volume 2: Ageing and Dynamical Scaling Far from Equilibrium* (Springer, Heidelberg, 2010).
[35]D. S. Fisher and D. A. Huse, "Nonequilibrium dynamics of spin glasses," Phys. Rev. B **38**, 373 (1988).
[36]K. Humayun and A. J. Bray, "Non-equilibrium dynamics of the Ising model for $T \leq T_c$," J. Phys. A: Math. Gen. **24**, 1915 (1991).
[37]F. Liu and G. F. Mazenko, "Nonequilibrium autocorrelations in phase-ordering dynamics," Phys. Rev. B **44**, 9185 (1991).
[38]M. Henkel, M. Pleimling, C. Godrèche, and J.-M. Luck, "Aging, phase ordering, and conformal invariance," Phys. Rev. Lett. **87**, 265701 (2001).

[39]M. Henkel, A. Picone, and M. Pleimling, "Two-time autocorrelation function in phase-ordering kinetics from local scale invariance," Europhys. Lett. **68**, 191 (2004).

[40]E. Lorenz and W. Janke, "Numerical tests of local scale invariance in ageing q-state Potts models," Europhys. Lett. **77**, 10003 (2007).

[41]J. Midya, S. Majumder, and S. K. Das, "Aging in ferromagnetic ordering: Full decay and finite-size scaling of autocorrelation," J. Phys.: Condens. Matter **26**, 452202 (2014).

[42]J. Midya, S. Majumder, and S. K. Das, "Dimensionality dependence of aging in kinetics of diffusive phase separation: Behavior of order-parameter autocorrelation," Phys. Rev. E **92**, 022124 (2015).

[43]C. Yeung, M. Rao, and R. C. Desai, "Bounds on the decay of the autocorrelation in phase ordering dynamics," Phys. Rev. E **53**, 3073 (1996).

[44]M. Bachmann and W. Janke, "Thermodynamics of lattice heteropolymers," J. Chem. Phys. **120**, 6779 (2004).

[45]G. Subramanian and S. Shanbhag, "On the relationship between two popular lattice models for polymer melts," J. Chem. Phys. **129**, 144904 (2008).

[46]A. M. Ferrenberg and R. H. Swendsen, "Optimized Monte Carlo data analysis," Phys. Rev. Lett. **63**, 1195 (1989).

[47]W. Janke, "Histograms and all that," in *Computer Simulations of Surfaces and Interfaces*, NATO Science Series, edited by B. Dünweg, D. P. Landau, and A. I. Milchev (Springer, Berlin, 2003), Vol. 114, pp. 137–157.

[48]J. M. Polson and M. J. Zuckermann, "Simulation of short-chain polymer collapse with an explicit solvent," J. Chem. Phys. **116**, 7244 (2002).

[49]B. Efron, *The Jackknife, the Bootstrap and Other Resampling Plans* (Society for Industrial and Applied Mathematics, Philadelphia, PA, 1982).

[50]B. Efron and R. J. Tibshirani, *An Introduction to the Bootstrap* (Springer Science+Business Media, Dordrecht, 1994).

[51]M. T. Gurler, C. C. Crabb, D. M. Dahlin, and J. Kovac, "Effect of bead movement rules on the relaxation of cubic lattice models of polymer chains," Macromolecules **16**, 398 (1983).

[52]S. Majumder and S. K. Das, "Domain coarsening in two dimensions: Conserved dynamics and finite-size scaling," Phys. Rev. E **81**, 050102 (2010).

[53]S. Majumder and S. K. Das, "Diffusive domain coarsening: Early time dynamics and finite-size effects," Phys. Rev. E **84**, 021110 (2011).

[54]S. Majumder and S. K. Das, "Temperature and composition dependence of kinetics of phase separation in solid binary mixtures," Phys. Chem. Chem. Phys. **15**, 13209 (2013).

[55]T. Komori, H. Yoshino, and H. Takayama, "Numerical study on aging dynamics in the 3D Ising spin-glass model. I. Energy relaxation and domain coarsening," J. Phys. Soc. Jpn. **68**, 3387 (1999).

[56]O. G. Mouritsen, "Temperature-dependent domain-growth kinetics of orientationally ordered phases: Effects of annealed and quenched vacancies," Phys. Rev. B **32**, 1632 (1985).

[57]R. Paul, S. Puri, and H. Rieger, "Domain growth in random magnets," Europhys. Lett. **68**, 881 (2004).

[58]R. Paul, S. Puri, and H. Rieger, "Domain growth in Ising systems with quenched disorder," Phys. Rev. E **71**, 061109 (2005).

[59]R. Paul, G. Schehr, and H. Rieger, "Superaging in two-dimensional random ferromagnets," Phys. Rev. E **75**, 030104 (2007).

[60]M. E. Fisher, "The theory of critical point singularities," in *Critical Phenomena, Proceedings of the 51st Enrico Fermi Summer School, Varenna*, edited by M. S. Green (Academic, New York, 1971), pp. 1–99.

[61]S. K. Das, S. Roy, S. Majumder, and S. Ahmad, "Finite-size effects in dynamics: Critical vs. coarsening phenomena," Europhys. Lett. **97**, 66006 (2012).

[62]S. Majumder and W. Janke, "Aging and related scaling during the collapse of a polymer," J. Phys.: Conf. Ser. **750**, 012020 (2016).

[63]H. Park and M. Pleimling, "Aging in coarsening diluted ferromagnets," Phys. Rev. B **82**, 144406 (2010).

[64]J. Kurchan, "Elementary constraints on autocorrelation function scalings," Phys. Rev. E **66**, 017101 (2002).

[65]L. Ramos and L. Cipelletti, "Ultraslow dynamics and stress relaxation in the aging of a soft glassy system," Phys. Rev. Lett. **87**, 245503 (2001).

[66]E. Pitard and J.-P. Bouchaud, "Glassy effects in the swelling/collapse dynamics of homogeneous polymers," Eur. Phys. J. E **5**, 133 (2001).

[67]N. V. Dokholyan, E. Pitard, S. V. Buldyrev, and H. E. Stanley, "Glassy behavior of a homopolymer from molecular dynamics simulations," Phys. Rev. E **65**, 030801 (2002).

[68]More generally one uses the scaling form $C(t, t_w) = C_s(t_w)^{-bz} f(C_s(t)/C_s(t_w))$, where the non-trivial exponent b is *a priori* unknown. For our system, however, we find $b = 0$.

[69]N. Clisby, "Accurate estimate of the critical exponent ν for self-avoiding walks via a fast implementation of the pivot algorithm," Phys. Rev. Lett. **104**, 055702 (2010).

[70]K. A. Dill, "Theory for the folding and stability of globular proteins," Biochemistry **24**, 1501 (1985).